View metadata, citation and similar papers at core.ac.uk

brought to you by CORE

provided by DSpace@MIT

Check for updates

Sulfur monoxide thermal release from an anthracene-based precursor, spectroscopic identification, and transfer reactivity

Maximilian Joost[a], Matthew Nava[a], Wesley J. Transue[a], Marie-Aline Martin-Drumel[b], Michael C. McCarthy[c], David Patterson[d,1], and Christopher C. Cummins[a,2]

[a]Department of Chemistry, Massachusetts Institute of Technology, Cambridge, MA 02139; [b]Institut des Sciences Moléculaires d'Orsay, CNRS, Université Paris–Sud, Université Paris-Saclay, 91405 Orsay, France; [c]Harvard-Smithsonian Center for Astrophysics, Atomic and Molecular Physics Division, Cambridge, MA 02138; and [d]Department of Physics, Harvard University, Cambridge, MA 02138

Contributed by Christopher C. Cummins, April 19, 2018 (sent for review March 8, 2018); reviewed by Norman C. Craig and Douglas W. Stephan)

Sulfur monoxide (SO) is a highly reactive molecule and thus, eludes bulk isolation. We report here on synthesis and reactivity of a molecular precursor for SO generation, namely 7-sulfinylamino-7-azadibenzonorbornadiene (1). This compound has been shown to fragment readily driven by dinitrogen expulsion and anthracene formation on heating in the solid state and in solution, releasing SO at mild temperatures (<100 °C). The generated SO was detected in the gas phase by MS and rotational spectroscopy. In solution, 1 allows for SO transfer to organic molecules as well as transition metal complexes.

microwave spectroscopy | reactive intermediate | molecular precursor | astrochemistry | sulfur monoxide

In contrast to the ubiquitous and well-studied chemistry of earth-abundant dioxygen (1), the chemistry of its heavier, valence-isoelectronic analogue sulfur monoxide (SO) is hardly explored and has been relegated to a niche existence, which is certainly due to its high reactivity: SO is unstable under ambient conditions toward disproportionation to SO_2 and elemental S (2) and eludes bulk isolation. However, in space, SO can accumulate and has been found in the interstellar medium (3, 4) as well as in our solar system (5–7), which is important to note considering that both O and S are biogenic elements (8).

Fragmentation of suitable molecular precursors presents a potential entry point to explore the synthetic chemistry for such reactive species and opens new avenues for spectroscopic characterization (9–16). In the case of SO, a limited number of synthetic precursors have been reported that allow thermal transfer of SO (Fig. 1): well-investigated are the chemistries of episulfoxides (**A**) (17–20), a thiadiazepin *S*-oxide (**B**) (21), trisulfide oxides (**C**) (22, 23), thianorbornadiene-*S*-oxides (**D**) (24), and *N*-sulfinylamine phosphinoborane adducts (**E**) (25). In explaining the SO transfer reactions of some of these substances, the intermediacy of free SO is assumed, while for others, the precursors fragment likely via associative mechanisms.

Our group has a longstanding interest in small reactive species, such as P_2 (9–11), AsP (12), HCP (13), phosphinidenes (14, 15), and dimethylgermylene (16), generated by mild thermal activation of suitable precursors. The driving force of anthracene ($C_{14}H_{10}$, **A**) expulsion for the release of highly reactive molecules and subsequent characterization and synthetic transfer has been amply capitalized on (13, 14, 26–31). Against this backdrop and our reasoning that an additional N_2 unit should further increase the energy of the ground state of the precursor molecule, we envisioned our synthetic target, 7-sulfinylamino-7-azadibenzonorbornadiene, OSN_2**A** (**1**), as promising for SO release simultaneously with **A** and dinitrogen formation. To probe this hypothesis, we compared the computed Gibbs free energies for singlet SO release from *A*–*E* and **1** (Fig. 1). Indeed, the formation of singlet SO was predicted to be thermodynamically strongly favorable only in case of **1**.

Free SO, amenable to spectroscopy, has been generated by electric discharge experiments of SO-containing gases (OCS, SO_2) (32) or using ethylene episulfoxide at high temperature (180 °C to 580 °C) (33). To the best of our knowledge, spectroscopic observation of free SO provided by mild thermolysis of a well-defined, solid, and easy-to-handle precursor compound has not been achieved. With **1**, we present now the synthesis of such a compound that fragments at approximately 95 °C in the solid state and allows for direct detection of SO in the gas phase. In addition, examples of SO transfer with this reagent in solution to both organic molecules and transition metal complexes are outlined.

Results and Discussion

The synthesis of **1** was achieved by reaction of Carpino's hydrazine (7-amino-7-azadibenzonorbornadiene, H_2N_2**A**) (30) with thionyl chloride in the presence of triethyl amine (Scheme 1) (34).

Compound **1** was isolated as a pale yellow solid in very good yield (83%). In solution (benzene-d_6), the ^{1}H NMR chemical shift of the bridgehead protons at $\delta = 6.22$ ppm, located 1.48 ppm downfield from that of H_2N_2**A**, is reflective of the strongly withdrawing effect of the sulfinyl group. Colorless crystals grew from a concentrated toluene solution of **1** layered with diethyl ether at −35 °C and were subjected to X-ray diffraction analysis.

Significance

The generation of highly reactive molecules under controlled conditions is desirable, as it allows exploration of synthetic chemistry and enables spectroscopic studies of such elusive species. We report here on the synthesis and reactivity of a precursor molecule that readily fragments with concomitant expulsion of dinitrogen and anthracene to release the highly reactive sulfur monoxide, a compound of interest for both synthetic chemists and astrochemists.

Author contributions: M.J., M.N., W.J.T., and C.C.C. designed research; M.J., M.N., W.J.T., M.-A.M.-D., M.C.M., and D.P. performed research; M.J., M.N., W.J.T., M.-A.M.-D., M.C.M., and D.P. analyzed data; and M.J., M.N., W.J.T. and C.C.C. wrote the paper.

Reviewers: N.C.C., Oberlin College; and D.W.S., University of Toronto.

The authors declare no conflict of interest.

Published under the PNAS license.

Data deposition: The crystallography, atomic coordinates, and structure factors have been deposited in the Cambridge Structural Database to www.ccdc.cam.ac.uk/Solutions/CSDSystem/Pages/CSD.aspx (accession nos. 1567576 and 1567577).

[1]Present address: Department of Physics, University of California, Santa Barbara, CA 93106.

[2]To whom correspondence should be addressed. Email: ccummins@mit.edu.

This article contains supporting information online at www.pnas.org/lookup/suppl/doi:10.1073/pnas.1804035115/-/DCSupplemental.

Published online May 17, 2018.

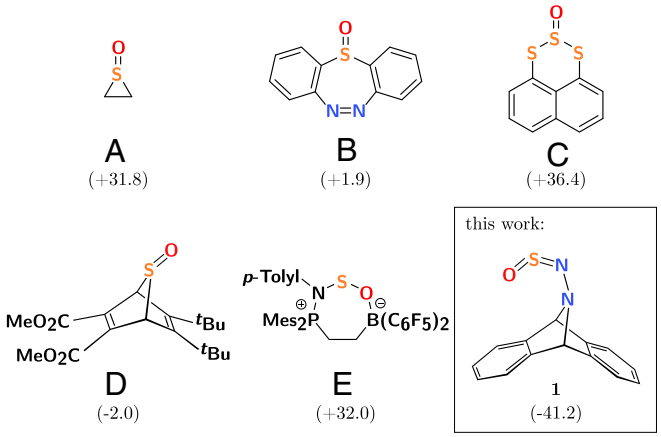

Fig. 1. Selection of previously reported compounds capable of SO transfer (*A–E*) and the anthracene-based sulfinylhydrazine **1** described herein. Computed Gibbs free energies (in kilocalories·mole^{-1} at 298.15 K; the density functional theory calculations were performed using the B3LYP-D3BJ functional and Def2-TZVP basis set) for singlet SO loss and formation of the respective coproducts are shown in parentheses.

The metrical data of the NNSO chain of **1** in the solid state (Fig. 2) compare well with the reported structures of sulfinyl hydrazines (35–37). One bridgehead proton of the azanorbornadiene scaffold weakly interacts with the terminal oxygen atom, leading to a synperiplanar NNSO arrangement as observed for $^{i}Pr_2N_2SO$ (36).

A thermogravimetric analysis (TGA) was performed to probe the potential release of SO. At 95 °C, a mass loss event of 30 wt % was observed, supporting the notion that N_2 and SO (11 and 19 wt %, respectively) were released (*SI Appendix*).

Eager to confirm the evolution of SO from **1** in accordance with the TGA experiment, direct spectroscopic observation of SO was sought. Detection of SO is difficult in condensed media and the gas phase due to its rapid self-reaction culminating in the formation of SO_2 and polysulfides (Eq. **1**) (2, 38, 39):

$$\begin{aligned} &2SO \rightleftharpoons S_2O_2 \\ &S_2O_2 + SO \rightarrow SO_2 + S_2O. \\ &2S_2O \rightarrow SO_2 + S_3 \end{aligned} \qquad [1]$$

Due to the propensity for self-reaction, SO is typically only generated and observed in high vacuum to minimize bimolecular reactivity, and accordingly, previous studies of molecular precursors for SO in condensed media relied on chemical trapping experiments and kinetic analysis to infer its intermediacy.

Thermolysis in a gas IR cell under static vacuum (approximately 50 mtorr) led to the identification of SO_2 as the major gaseous product in accord with loss of SO and subsequent disproportionation chemistry; however, it did not provide conclusive evidence for the intermediacy of SO (*SI Appendix*).

For the detection of such short-lived species on thermal decomposition of molecular precursors, molecular beam MS (MBMS) has proven to be a valuable tool to analyze unstable gaseous products evolved from molecular precursors (10, 13, 15). In case of thermolysis of **1** in the MBMS sample chamber, **A**, N_2, and SO were observed (Fig. 3). The differing results of the MBMS and gas IR experiments can be rationalized based on differences in pressure when **1** is thermolyzed and the large disparity in the rate of data acquisition between the two methods (IR spectrum acquisition required several seconds).

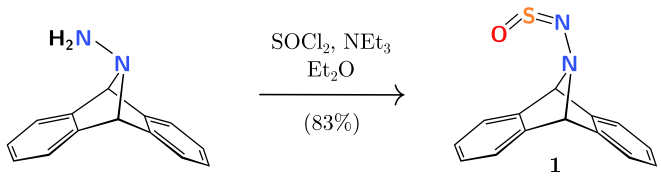

Scheme 1. Synthesis of **1**.

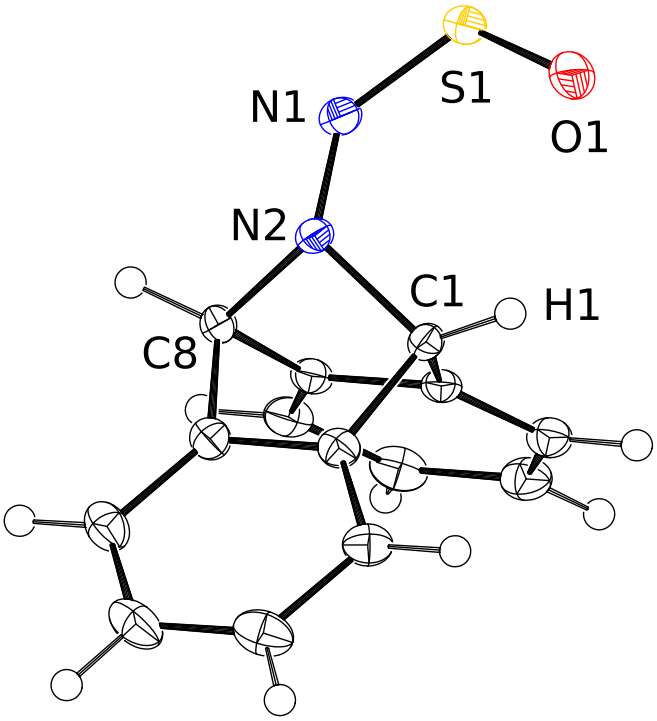

Fig. 2. Molecular structure of **1** in the solid state with thermal ellipsoids at the 50% probability level. Selected distances (angstroms) and angles (degrees): N1-N2 1.353(3), N1-S1 1.544(2), S1-O1 1.466(2), O1-H1 2.432 (intramolecular), H1-O1 2.489 (intermolecular), N2-N1-S1 125.9(2), N1-S1-O1 118.2(1), S1-O1-H1 100.0, C1-N2-C8 96.0(2).

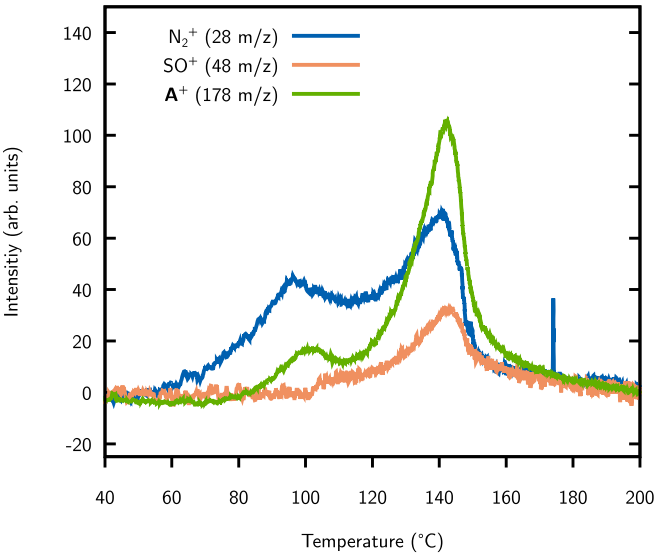

Fig. 3. MBMS of **1**.

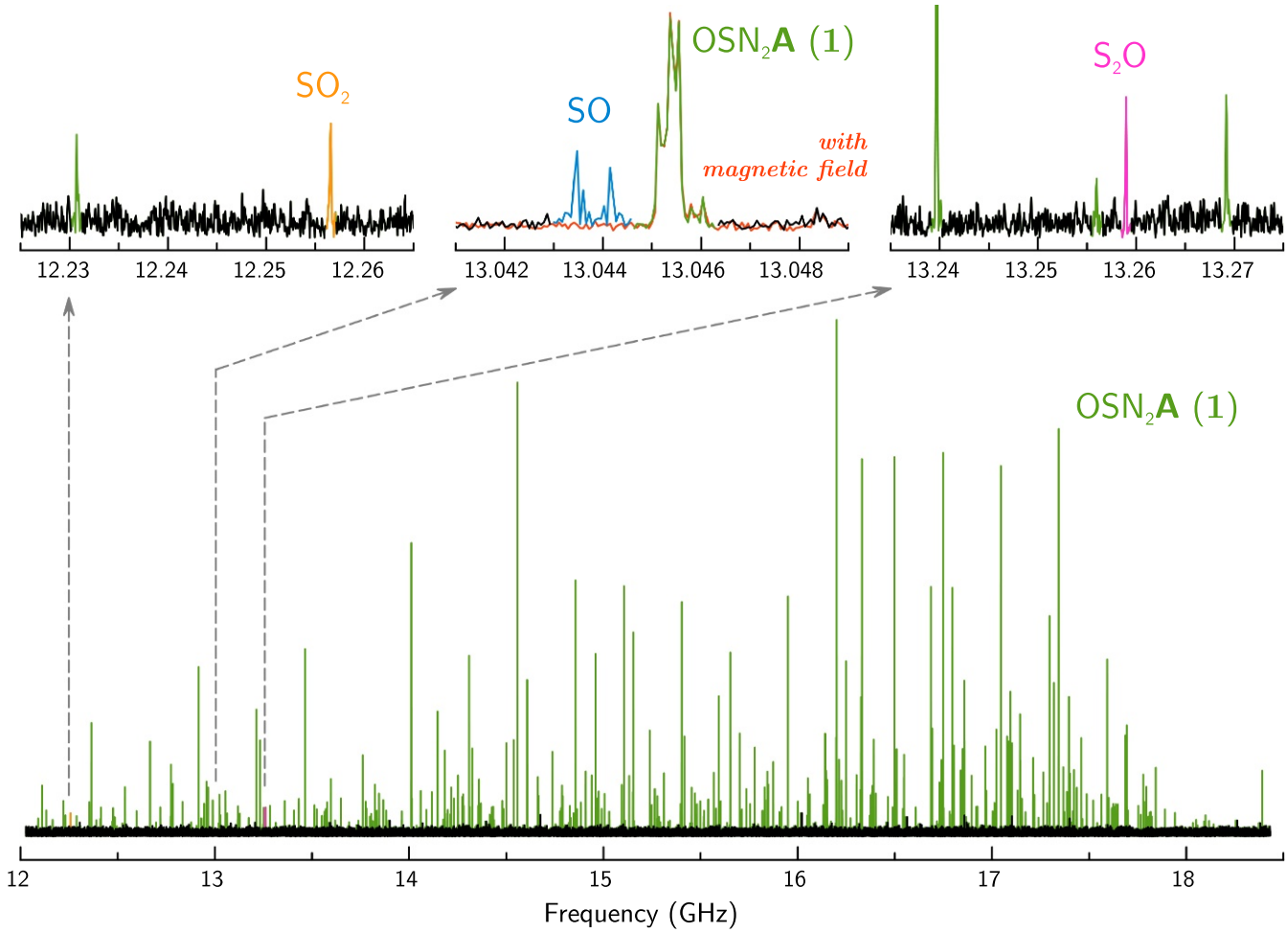

Fig. 4. Microwave spectrum of the compounds released during the thermal heating of **1**. Transitions belonging to **1**, SO_2, SO, and S_2O are indicated in green, orange, blue, and pink, respectively, and the black portions depict baseline and a few unassigned lines. The spectrum showing the SO transition was the result of a deeper integration, and an additional spectrum was recorded in the same conditions but under the influence of an external magnetic field (red) to confirm the open shell nature of the carrier of the lines assigned to SO. In presence of the magnetic field, lines of SO are not visible (as expected for a species with unpaired electrons in a $^3\Sigma$ ground electronic state), while the transitions of **1** (closed shell) are unaffected.

The direct observation of SO via MS encouraged us to attempt its characterization by microwave spectroscopy as well. The rotational transitions of SO have been previously studied in detail for ground electronic as well as the first excited state (40, 41). Compound **1** was thermolyzed in a specially constructed solid sample holder directed at the entrance of a buffer-gas cell (42). Gases evolved from **1** during heating enter the buffer-gas cell, where they collide with gaseous helium at approximately 10 K. The collisions of the evolved gases with the helium rapidly cool the molecules, which results in the rotational and vibrational cooling of the sample, simplifying their rotational spectra but also inhibiting bimolecular reactivity. After introduction and cooling of the fragment molecules, a microwave spectrum of the mixture was recorded (Fig. 4).

Next to characteristic transitions corresponding to S_2O ($2_{1,2} \leftarrow 3_{0,3}$; 13,258.94 MHz) (43) and SO_2 ($1_{1,1} \leftarrow 2_{0,2}$; 12,256.58 MHz) (44), $^3\Sigma^-$ SO ($1_2 \leftarrow 1_1$; 13,043.7 MHz) (40) was detected. As for O_2, the triplet ($^3\Sigma^-$) is the lowest-energy configuration for SO, with the closed shell ($^1\Delta$) and open shell ($^1\Sigma^+$) singlets lying 18.2 kcal·mol^{-1} (1 kcal = 4.18 kJ) and 30.1 ·mol^{-1} above the ground state, respectively (45). The transition for $^3\Sigma^-$ SO was split due to Earth's magnetic field and disappeared out of the spectral window in the presence of a strong external magnetic field. We are unable to verify the presence of the closed shell singlet SO, because the lowest-frequency transition at 42,591.23 MHz is out of range of the microwave instrument used (12,000–17,500 MHz) (46). The observation of open shell and closed shell singlet electronic states of SO should be feasible

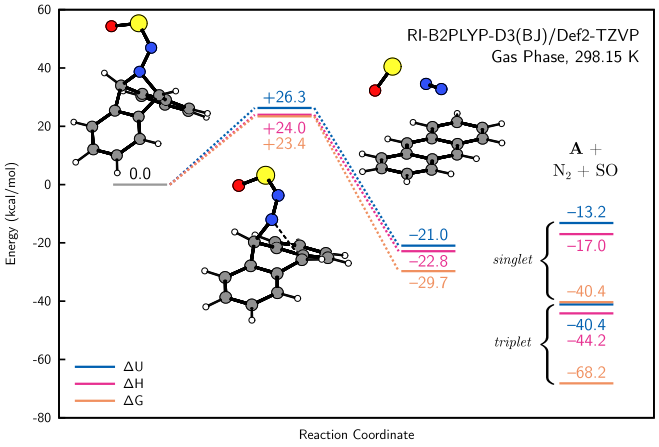

Fig. 5. Computed mechanism for the fragmentation of **1** as revealed by quantum chemical calculations carried out using the RI-B2PLYP-D3(BJ) density functional and the Def2-TZVP basis set.

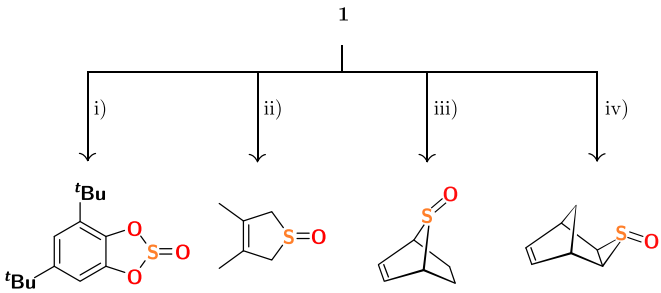

Scheme 2. Transfer of SO from **1**: (*i*) 3,5-di-*tert*-butyl-1,2-quinone (1 eq), benzene, 70 °C, 24 h (quantitative); (*ii*) DMB (neat), 80 °C, 16 h (60%); (*iii*) 1,3-cyclohexadiene (5 eq), benzene, 70 °C, 24 h (59%); (*iv*) norbornadiene (10 eq), benzene, 25 °C, 16 h (55%).

in principle: the radiative lifetimes of these species were determined to be approximately 7 ms (exp. value; calculated 13.6 ms) and 450 ms (calculated), respectively (47, 48). Singlet SO is thus sufficiently long-lived for detection with our apparatus with an approximate flight time of 2–3 ms assuming a reasonable molecular velocity in the gas phase (*SI Appendix*). However, an additional complication is the propensity of singlet SO for collisional relaxation to the $^3\Sigma^-$ spin state with third bodies, such as the heated walls of the sample holder (49).

In addition, we were able to identify the rotational transitions of **1** itself, which partially transferred without fragmentation into the gas phase. The pure rotational spectrum of **1** was analyzed using a variant of the Automated Microwave Double Resonance technique (50). The small differences between the experimentally obtained rotational constants and those recovered from calculations based on the geometry of **1** in the crystal structure imply that the structure of **1** is nearly identical in the solid state and in the gas phase (*SI Appendix*). The differences in the observed products of thermolysis of **1** highlight the complementary nature of the techniques used but also illustrate how critical the thermolysis conditions are to what gases are evolved from **1**.

To comment on the thermolysis mechanism of **1**, quantum chemical calculations were carried out using the RI-B2PLYP-D3(BJ) density functional and the Def2-TZVP basis set. A single-step fragmentation with concerted loss of singlet SO and N_2 from the anthracene platform was found, featuring a single transition state corresponding to the breaking of the C–N bond opposed to the sulfinylamino moiety. The minimum energy path across this transition state revealed no further stationary points en route to the final products: the structure collapsed in a concerted, asynchronous way with breaking of the N–S and of the second C–N bond. This is likely due to the NNSO intermediate not being a minimum on the potential energy surface (51). This quasisimultaneous breaking and making of bonds in this fragmentation process may be classified as a coarctate reaction as defined by Herges (52). While for pericyclic reactions, the concerted breaking and forming of bonds occur in a cyclic manner, coarctate processes describe bond rearrangements with a transition-state topology of a constricted cycle. The constriction point is located at the coarctate atom(s) at which two bonds are broken and reformed in the transition state. In case of the fragmentation of **1**, both N atoms are coarctate atoms. In this process, SO may indeed be released in its singlet state: the formation of **A**, N_2, and singlet SO is favored by -40.4 kcal·mol^{-1} with respect to the starting material (Fig. 5).

With evidence of SO release on thermolysis in the solid state, we explored the reactivity of **1** in solution. Heating **1** in benzene-d_6 in a sealed tube led to its decomposition, which was indicated visually by a color change from colorless to yellow likely due to production of sulfur. The sole product observable by ^{1}H NMR spectroscopy was **A**. This reaction obeyed a first-order rate law with $k_{\mathrm{obs}} = (2.743 \pm 0.436) \times 10^{-4}$ s^{-1} at 80 °C in THF as determined by ultraviolet–visible spectroscopy. This barrier corresponded to an activation barrier of $\Delta G^{\ddagger}(80\,^{\circ}\mathrm{C}) = 26.55(11)$ kcal·mol^{-1} according to the Eyring equation, similar to the calculated value of $\Delta G^{\ddagger}_{\mathrm{calc}}(80\,^{\circ}\mathrm{C}) = 23.3$ kcal·mol^{-1}.

To assess the possibility of SO transfer from **1** to an acceptor, various representative reaction partners were used. We focused first on organic compounds suitable for SO trapping, such as quinones and olefins (Scheme 2). Compound **1** was heated with 3,5-di-*tert*-butyl-1,2-quinone for 24 h to 70 °C to convert quantitatively to the corresponding known sulfite (53).

Several SO-releasing precursors are capable of SO addition to 1,3-dienes (18, 21–24, 54, 55). Heating of **1** with an excess (5 eq) of 2,3-dimethyl-1,3-butadiene (DMB) led to decomposition of **1** without thiophene-*S*-oxide formation. However, when performing the reaction at 80 °C in neat DMB, this SO transfer product was observed (60%). Similarly, transfer of SO to 1,3-cyclohexadiene was successful. Likely due to the locked *cisoid* conformation of the double bond, just a fivefold excess of this diene was sufficient to lead to formation of 7-oxo-7-thianorbornene (59%) (23). Thermal SO transfer to other olefins or alkynes was unsuccessful: reactions using *cis*-stilbene, styrene,

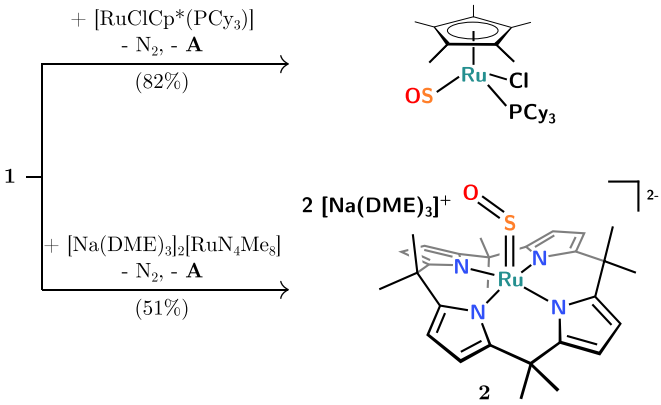

Scheme 3. Transfer of SO from **1** to ruthenium complexes.

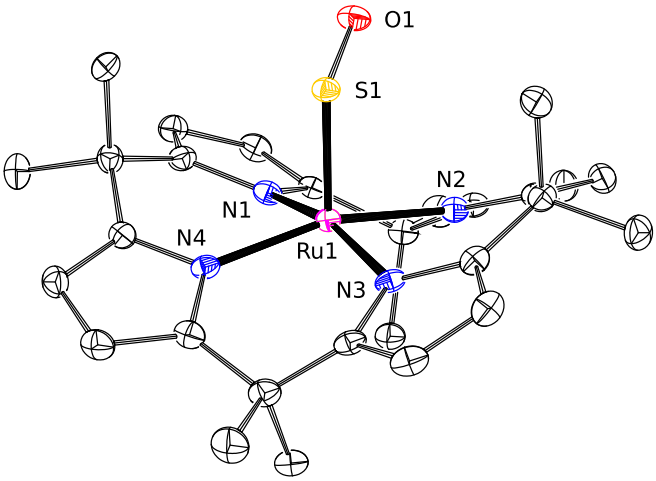

Fig. 6. Molecular structure of **2** in the solid state with thermal ellipsoids at the 50% probability level. SO-coordinated sodium cation and separate sodium tris(1,2-dimethoxyethane) cation as well as one cocrystallized THF solvent molecule have been omitted for clarity. Selected distances (angstroms) and angles (degrees): Ru1-S1 2.0282(8), S1-O1 1.503(2), Ru1-N 2.044 (average); Ru1-S1-O1 118.17(11).

or phenyl acetylene in excess did not provide the respective addition products. Contrasting reactivity of **1** toward norbornadiene yielded the corresponding thiirane (55%): addition of SO occurred at 25 °C (16 h), well below the temperature required for fragmentation of **1**, and thus, it does not involve free SO but rather, proceeds via an associative mechanism. The SO transfer from **1** to transition metal complexes also occurs through an associative mechanism (Scheme 3). Stirring a solution of **1** and $[RuCl(Cp^*)(PCy_3)]$ ($Cp^* = \eta^5$-C_5Me_5) in THF at 25 °C for 30 min led to a gradual color change from blue to red–brown. After removal of **A**, the known SO ruthenium complex $[RuCl(Cp^*)(SO)(PCy_3)]$ was isolated (82%) (56, 57). Compound **1** also reacted with the anionic ruthenium complex $[Na(DME)_3]_2$ $[Ru(N_4Me_8)]$ ($H_4N_4Me_8$ = octamethylporphyrinogen) (58) to give $[Na(DME)_3][Ru(N_4Me_8)(SO)]$ (**2**), obtained in 51% yield after removal of anthracene and selective crystallization as a brown–orange solid.

Cooling a solution of this compound in THF and DME to −35 °C yielded dark orange crystalline blocks. An X-ray diffraction analysis revealed a dimeric structure, with sodium ions bridging two units of the $[Ru(N_4Me_8)(SO)]^{2-}$ platform (Fig. 6). These units feature the ruthenium center in a square-pyramidal environment, in which the SO ligand occupies the apical position. The Ru–S bond [2.0282(8) Å] is slightly shorter and the S–O bond [1.503(2) Å] is slightly longer than in a related Ru(II)-SO complex [2.0563(11) and 1.447(3) Å, respectively] (59). Terminal SO transition metal complexes generally show a strong SO stretch around 1,046–1,126 cm^{-1} (55, 56, 59, 60). Analysis of the IR spectrum of **2** revealed a band at 1,021 cm^{-1} assigned to the SO stretching vibration. Both this notable red shift with regard to values for related compounds as well as the metrical data for **2** are in accord with strong backbonding from Ru to the SO ligand due to the electron-rich porphyrinogen ligand. Coordination of the sodium cations to the oxygen atom of ligated SO may enhance this effect.

We did not observe selective reaction of **1** with *N*-heterocyclic carbenes to give the corresponding sulfines. However, heating a mixture of **1** and a phosphine (PPh_3 or P^tBu_3) in benzene gave about equimolar mixtures of the respective phosphine oxides and phosphine sulfides via formal splitting of SO (25).

Conclusion

We have shown here a well-controlled synthetic route to SO by thermal decomposition of **1**. Taking reactivity, computational studies, and spectroscopic detection of $^3\Sigma^-$ SO into consideration, it is believed that **1** generates $^1\Delta$ SO on thermolysis. $^3\Sigma^-$ SO is detected by microwave spectroscopy, possibly originating from a small amount of $^1\Delta$ SO that has had enough time to phosphoresce into the lower-energy triplet ground state. Regardless of the spin state of the SO evolved from **1**, this study firmly establishes that SO is in fact released from the molecular precursor, illustrating the power of synthesis in combination with spectroscopy to shed light on reactive intermediates of general importance.

Methods

Experimental and computational details and crystallographic information are included in *SI Appendix*. Computed atomic coordinates are included in Datasets S1–S4.

ACKNOWLEDGMENTS. We thank Prof. Robert Field (Massachusetts Institute of Technology) for inspiring discussions. This material is based on research supported by National Science Foundation (NSF) Grant CHE-1664799. M.J. thanks the Alexander von Humboldt Foundation for a Feodor Lynen Postdoctoral Fellowship. D.P. acknowledges support from NSF Instrument Development for Biological Research Program NSF Award 134076–5101408.

1. Wiberg E, Wiberg N, Holleman AF (2001) *Inorganic Chemistry* (Academic, San Diego).
2. Herron JT, Huie RE (1980) Rate constants at 298 K for the reactions SO+SO+M→(SO) $_2$+M and SO+(SO)$_2$ →SO$_2$+S$_2$O. *Chem Phys Lett* 76:322–324.
3. Gottlieb CA, Gottlieb EW, Litvak MM, Ball JA, Penfield H (1978) Observations of interstellar sulfur monoxide. *Astrophys J* 219:77–94.
4. Sakai N, et al. (2014) Change in the chemical composition of infalling gas forming a disk around a protostar. *Nature* 507:78–80.
5. Na CY, Esposito LW, Skinner TE (1990) International Ultraviolet Explorer observation of Venus SO2 and SO. *J Geophys Res* 95:7485–7491.
6. Russell CT, Kivelson MG (2000) Detection of SO in Io's Exosphere. *Science* 287:1998–1999.
7. Boissier J, et al. (2007) Interferometric imaging of the sulfur-bearing molecules H_2S, SO, and CS in comet C/1995 O1 (Hale-Bopp). *Astron Astrophys* 475:1131–1144.
8. National Research Council (1990) *The Search for Life's Origins: Progress and Future Directions in Planetary Biology and Chemical Evolution* (National Academies, Washington, DC), pp 21–55.
9. Piro NA, Figueroa JS, McKellar JT, Cummins CC (2006) Triple-bond reactivity of diphosphorus molecules. *Science* 313:1276–1279.
10. Velian A, et al. (2014) A retro Diels–Alder route to diphosphorus chemistry: Molecular precursor synthesis, kinetics of P_2 transfer to 1,3-dienes, and detection of P2 by molecular beam mass spectrometry. *J Am Chem Soc* 136:13586–13589.
11. Velian A, Cummins CC (2015) Synthesis and characterization of P_2N_3-: An aromatic ion composed of phosphorus and nitrogen. *Science* 348:1001–1004.
12. Spinney HA, Piro NA, Cummins CC (2009) Triple-bond reactivity of an AsP complex intermediate: Synthesis stemming from molecular arsenic, As_4. *J Am Chem Soc* 131:16233–16243.
13. Transue WJ, et al. (2016) A molecular precursor to phosphaethyne and its application in synthesis of the aromatic 1,2,3,4-phosphatriazolate anion. *J Am Chem Soc* 138:6731–6734.
14. Velian A, Cummins CC (2012) Facile synthesis of Dibenzo-7λ^3-phosphanorbornadiene derivatives using magnesium anthracene. *J Am Chem Soc* 134:13978–13981.
15. Transue WJ, et al. (2017) On the mechanism and scope of phosphinidene transfer from Dibenzo-7-phosphanorbornadiene compounds. *J Am Chem Soc* 139:10822–10831.
16. Velian A, Transue WJ, Cummins CC (2015) Synthesis, characterization, and thermolysis of Dibenzo-7-dimethylgermanorbornadiene. *Organometallics* 34:4644–4646.
17. Hartzell GE, Paige JN (1966) Ethylene episulfoxide. *J Am Chem Soc* 88:2616–2617.
18. Dodson RM, Sauers RF (1967) Sulphur monoxide: Reaction with dienes. *Chem Commun*, 1189–1190.
19. Abu-Yousef IA, Harpp DN (1995) A useful precursor for sulfur monoxide transfer. *Tetrahedron Lett* 36:201–204.
20. Abu-Yousef IA, Harpp DN (1997) Effective precursors for sulfur monoxide formation. *J Org Chem* 62:8366–8371.
21. Chow YL, Tam JNS, Blier JE, Szmant HH (1970) Mechanism of sulphur monoxide extrusion. *J Chem Soc D*, 1604–1605.
22. Grainger RS, Procopio A, Steed JW (2001) A novel recyclable sulfur monoxide transfer reagent. *Org Lett* 3:3565–3568.
23. Grainger RS, Patel B, Kariuki BM, Male L, Spencer N (2011) Sulfur monoxide transfer from peri-substituted trisulfide-2-oxides to dienes: Substituent effects, mechanistic studies and application in thiophene synthesis. *J Am Chem Soc* 133:5843–5852.
24. Nakayama J, Tajima Y, Xue-hua P, Sugihara Y (2007) [1 + 2] Cycloadditions of sulfur monoxide (SO) to alkenes and alkynes and [1 + 4] cycloadditions to dienes (polyenes). Generation and reactions of singlet SO? *J Am Chem Soc* 129:7250–7251.
25. Longobardi LE, Wolter V, Stephan DW (2015) Frustrated Lewis pair activation of an N-sulfinylamine: A source of sulfur monoxide. *Angew Chem Int Ed* 54:809–812.
26. Corey EJ, Mock WL (1962) Chemistry of diimide. III. Hydrogen transfer to multiple bonds by dissociation of the diimide-anthracene adduct, anthracene-9,10-biimine. *J Am Chem Soc* 84:685–686.
27. Wasserman HH, Scheffer JR (1967) Singlet oxygen reactions from photoperoxides. *J Am Chem Soc* 89:3073–3075.
28. Baldwin JE, Lopez RCG (1982) The generation and trapping of thiobenzaldehyde and thioacetaldehyde. *J Chem Soc Chem Commun* 1029–1030.
29. Appler H, Gross LW, Mayer B, Neumann WP (1985) Die chemie der schweren carbenanalogen R_2M, M = Si, Ge, Sn. *J Organomet Chem* 291:9–23.
30. Carpino LA, et al. (1988) Synthesis, characterization, and thermolysis of 7-Amino-7-azabenzonorbornadienes. *J Org Chem* 53:2565–2572.
31. Courtemanche MA, Transue WJ, Cummins CC (2016) Phosphinidene reactivity of a transient vanadium P≡N complex. *J Am Chem Soc* 138:16220–16223.
32. Sanz ME, McCarthy MC, Thaddeus P (2003) Rotational transitions of SO, SiO, and SiS excited by a discharge in a Supersonic molecular beam: Vibrational temperatures, Dunham coefficients, Born–Oppenheimer breakdown, and hyperfine structure. *J Chem Phys* 119:11715–11727.
33. Saito S (1969) Detection of sulfur monoxide in the pyrolysis of ethylene episulfoxide by microwave spectroscopy. *Bull Chem Soc Jpn* 42:667–670.
34. Michaelis A (1889) Über anorganische derivate des phenylhydrazins. *Ber Dtsch Chem Ges* 22:2228–2233.
35. Gieren A, Dederer B (1977) X-ray structure analysis of N-phenyl-N′-sulfinyl-hydrazine. *Angew Chem Int Ed* 16:179–180.
36. Cerioni G, Piras P, Marongiu G, Macciantelli D, Lunazzi L (1981) Conformational studies by dynamic nuclear magnetic resonance spectroscopy. Part 21. Structure, conformation, and stereodynamics of sulphinylhydrazines. *J Chem Soc Perkin Trans* 2:1449–1453.
37. Schanda F, Gieren A, Filhol A (1984) Refinement of the structure of N-phenyl-N′-sulfinylhydrazine, $C_6H_6N_2OS$, at 120(1) K with neutron data. *Acta Crystallogr Sect C Cryst Struct Commun* 40:306–308.

38. Nakayama J, et al. (2004) Reversible disulfur monoxide (S_2O)-forming retro-Diels-Alder reaction. Disproportionation of S_2O to trithio-Ozone (S_3) and sulfur dioxide (SO_2) and reactivities of S2O and S3. *J Am Chem Soc* 126:9085–9093.
39. Meschi DJ, Myers RJ (1956) Disulfur monoxide. I. Its identification as the major constituent in Schenk's "sulfur monoxide." *J Am Chem Soc* 78:6220–6223.
40. Amano T, Hirota E, Morino Y (1967) Microwave spectrum of the SO radical. equilibrium S-O distance, electric quadrupole coupling constant and magnetic hyperfine structure constants. *J Phys Soc Jpn* 22:399–412.
41. Clark WW, De Lucia FC (1976) The microwave spectrum and rotational structure of the $^1\Delta$ and $^3\Sigma$ Electronic states of sulfur monoxide. *J Mol Spectrosc* 60:332–342.
42. Patterson D, Rasmussen J, Doyle JM (2009) Intense atomic and molecular beams via neon buffer-gas cooling. *New J Phys* 11:055018.
43. Thorwirth S, et al. (2006) Rotational spectroscopy of S_2O: Vibrational satellites, ^{33}S isotopomers, and the sub-millimeter-wave spectrum. *J Mol Struct* 795:219–229.
44. Ellenbroek AW, Dymanus A (1976) Zeeman effect in SO_2 by beam maser Zeeman spectroscopy. *Chem Phys Lett* 42:303–306.
45. Colin R (1968) The $b^1\Sigma^+$–$X^3\Sigma^-$ band system of SO. *Can J Phys* 46:1539–1546.
46. Müller HSP, Schlöder F, Stutzki J, Winnewisser G (2005) The Cologne Database for Molecular Spectroscopy, CDMS: A useful tool for astronomers and spectroscopists. *J Mol Struct* 742:215–227.
47. Wildt J, Fink EH, Winter R, Zabel F (1983) Radiative lifetime and quenching of SO($b^1\Sigma^+, v' = 0$). *Chem Phys* 80:167–175.
48. Klotz R, Marian CM, Peyerimhoff SD, Hess BA, Buenker RJ (1984) Calculation of spin-forbidden radiative transitions using correlated wavefunctions: Lifetimes of $b^1\Sigma^+$, $a^1\Delta$ States in O_2, S_2 and SO. *Chem Phys* 89:223–236.
49. Saito S (1969) Detection of sulfur monoxide in the pyrolysis of ethylene episulfoxide by microwave spectroscopy. *Bull Chem Soc Jpn* 42:667–670.
50. Martin-Drumel MA, McCarthy MC, Patterson D, McGuire BA, Crabtree KN (2016) Automated microwave double resonance spectroscopy: A tool to identify and characterize chemical compounds. *J Chem Phys* 144:124202.
51. Andrews L, Hassanzadeh P, Brabson GD, Citra A, Neurock M (1996) Reactions of nitric oxide with sulfur species. Infrared spectra and density functional theory calculations for SNO, SNO^+, SSNO, and SNNO in solid argon. *J Phys Chem* 100:8273–8279.
52. Herges R (2015) Coarctate and pseudocoarctate reactions: Stereochemical rules. *J Org Chem* 80:11869–11876.
53. Schenk WA, Leißner J (1987) Freisetzung von Schwefelmonoxid aus seinen Komplexverbindungen [1]. *Z Naturforsch B Chem Sci* 42:799–800.
54. Chao P, Lemal DM (1973) Sulfur monoxide chemistry. Stereochemistry of the thiirane oxide-diene reaction. *J Am Chem Soc* 95:920–922.
55. Heyke O, Neher A, Lorenz IP (1992) Bis(triphenylphosphan)Palladium-Komplexe mit Schwefeloxid-Liganden. *Z Anorg Allg Chem* 608:23–27.
56. Schenk WA, Karl U (1989) Chirale Ruthenium-Halbsandwichkomplexe des Schwefelmonoxids und Schwefeldioxids. *Z Naturforsch B Chem Sci* 44:988–989.
57. Schenk WA (2011) The coordination chemistry of small sulfur-containing molecules: A personal perspective. *Dalton Trans* 40:1209–1219.
58. Bonomo L, Solari E, Scopelliti R, Floriani C (2001) Ruthenium nitrides: Redox chemistry and photolability of the Ru–Nitrido group. *Angew Chem Int Ed* 40:2529–2531.
59. Leung WH, et al. (2000) Ruthenium complexes with $N(SPR_2)_2^-$ (R = Ph or Pr^i). *J Chem Soc, Dalton Trans*, 423–430.
60. Schenk WA, Leissner J, Burschka C (1984) Stabilization of sulfur monoxide by coordination to transition metals. *Angew Chem Int Ed* 23:806–807.

CHEMISTRY